RSC Advances

PAPER

Cite this: *RSC Adv.*, 2019, **9**, 40277

In situ deposition of MOF199 onto hierarchical structures of bamboo and wood and their antibacterial properties†

Minglei Su,[a] Rong Zhang,*[a] Huairui Li,[a] Xiaobei Jin,[a] Jingpeng Li,[b] Xianfeng Yue[a] and Daochun Qin[a]

Received 3rd September 2019
Accepted 21st November 2019

DOI: 10.1039/c9ra07046j

rsc.li/rsc-advances

Tremendous efforts have been dedicated to developing functionalized cellulose materials by synthesis with copper-based metal–organic frameworks (MOF199), also known as HKUST-1. However, few studies have explored the deposition of MOFs on woody materials due to the complex chemical compositions of these materials (cellulose, hemicellulose, lignin) and their difficulty of bonding with MOF crystals. In this article, for the first time, MOF199 was successfully synthesized onto two different woody materials, moso bamboo and balsa wood, *via in situ* deposition at room temperature. The results show that the diverse surface roughness and the hierarchical structures of woody materials have significant effects on the size of MOF199 crystal. Additionally, bamboo and wood coated with MOF199 exhibited better antibacterial activities against *Staphylococcus aureus* (*S. aureus*) than *Escherichia coli* (*E. coli*); they could minimize *S. aureus* colony levels to 2.08 from 8.98 CFU cm^{-2}. This study provides a facile method for the functionalization of woody materials with MOFs for antibacterial applications.

Introduction

As renewable biomass resources, timber and non-timber plants, including wood, bamboo, and shrubs, are widely used in industrial production and daily necessities.[1] Balsa wood (*Ochroma pyramidale*) is a fast-growing wood species with important development and application prospects.[2] Taking advantage of the lightweight, porous, hierarchical structure and thin-walled properties of balsa wood,[2] numerous studies have explored the development of advanced functional materials for energy-saving buildings,[3] conductive materials,[4] separation of oil/water[5] and solar steam generation.[6] Moso bamboo (*Phyllostachys edulis*) is the most important non-timber forest resource;[7] it is plentiful, inexpensive, and fast growing and has excellent physical and mechanical properties.[8,9] The hierarchical structures of balsa wood and moso bamboo are different. Wood is mainly composed of fiber, vessels and rays; meanwhile, bamboo mainly contains parenchyma and vascular bundles (fiber and vessels), and there is no lateral channeling tissue in bamboo. The different micromorphological characteristics of these materials may affect the formation or morphology of materials deposited on their surfaces. The chemical compositions of bamboo and wood are similar. Lignin is the most important component of cell walls in woody materials; it provides structural support, enables water transport, and contributes to plant defense mechanisms against both biotic and abiotic stresses.[10] Additionally, the cell wall is composed of cellulose (contains at least 40% to 50%) and some lower molecular weight polysaccharide chains (hemicellulose).[11] These compounds may act as nutrients for microbes and easily lead to bacterial infection, which is harmful to human health. Therefore, research on functional wood and bamboo with antibacterial properties is of vital importance.

Metal–organic framework materials (MOFs), which consist of metal ions with bridging organic linkers and have three-dimensional structures, are microporous and crystalline materials.[12] MOFs possess extremely high surface areas and pore volumes and regular pore structure sizes; as a result, they have been used in gas storage, heavy metal adsorption, antibacterial materials and catalysis.[13] A wide range of MOF crystals have been immobilized on cellulose fibers to obtain antibacterial properties. These textile products can be widely used for hygienic clothing, wound healing, and medical applications in hospitals and other places.[14] MOF199, which is water-stable, has been proved to possess powerful antibacterial activity by inducing damage to the bacterial envelope.[15–17] Abbasi *et al.* first reported the antimicrobial activity of MOF199 coated on silk against *Escherichia coli* (*E. coli*) and *Staphylococcus aureus* (*S. aureus*).[18] Further study by Rodríguez *et al.* found that a cellulose-MOF showed high antibacterial activity in both solid and liquid cultures, and copper ions did not leach from the coated fabric.[19] Wang *et al.* prepared a copper-based metal–organic

[a]*International Centre for Bamboo and Rattan, Beijing 100102, PR China. E-mail: zhangrong@icbr.ac.cn*

[b]*China National Bamboo Research Centre, Hangzhou 310012, PR China*

† Electronic supplementary information (ESI) available. See DOI: 10.1039/c9ra07046j

framework/cellulose fiber (MOF199/CF) composite *via* a DMF-free green process, and the synthetized MOF199/CF composite exhibited excellent antibacterial activity against *E. coli* and *S. aureus*.[12] In recent studies, MOF199/polymer electrospun fiber and MOF199/wool fabric were successfully prepared, and these materials exhibited excellent antibacterial effectiveness.[20] According to previous research, the deposition of MOFs is closely related to the cellulose fiber matrix; some of its polymers contain numerous hydroxyl groups and can readily chelate copper ions. However, few studies have explored the synthesis of MOFs on bamboo and wood, which have complex chemical compositions (lignin, cellulose and hemicellulose) and natural hierarchical structures. Considering that wood and bamboo are widely used in furniture, flooring, fabrics, crafts, *etc.*, it is increasingly necessary to develop functional wood and bamboo materials with antibacterial properties for health reasons.

Based on the recognized antibacterial ability of MOF199, for the first time, MOF199 is deposited on moso bamboo and balsa wood *in situ*. For the characterization of the obtained materials, X-ray diffraction (XRD), energy dispersive X-ray spectroscopy (EDS), FT-IR spectroscopy (FTIR), and scanning electron microscopy (SEM) were used. The differences in the surfaces of bamboo and wood and their effects on MOF deposition were studied by atomic force microscopy (AFM). The antibacterial properties of bamboo and wood-based MOF199 materials against *E. coli* and *S. aureus* were compared. The study in this article provides a new method for fabricating functionalized MOF-woody materials.

Experimental

Materials and chemicals

The four-year-old moso bamboo (*Phyllostachys edulis*) used in this study was obtained from Yongan, Fujian Province. The bamboo was processed into test samples with dimensions of 20 mm × 25 mm × 6 mm ($L \times T \times R$); balsa wood (*Ochroma pyramidale*) was purchased from Shanghai Haobei Model Company and prepared with dimensions of 20 mm × 25 mm × 8 mm ($L \times T \times R$). The two materials were both ultrasonically cleaned with deionized water and acetone for 30 min, then completely dried in an oven at 60 °C for 24 h. Copper nitrate trihydrate $Cu(NO_3)_2 \cdot 3H_2O$; 1,3,5-benzentricarboxylic acid (BTC, $C_6H_3(COOH)_3$); dimethyl sulfoxide (DMSO, C_2H_6SO); anhydrous methanol (CH_3OH); anhydrous ethanol (C_2H_5OH); and acetone (CH_3COCH_3) used in this study were purchased from Beijing Chemical Glass Station Biotechnology Company. All reagents and solvents were used without further purification.

In situ deposition of MOF199 on bamboo and wood surfaces

MOF199 was prepared according to a previous method;[21] in this article, the crystallization process was slightly adjusted, and the entire synthetic process was carried out at room temperature. The MOF199 precursor solution was prepared by dissolving copper(II) nitrate trihydrate (2.44 g) and 1,3,5-benzenetricarboxylic acid (1.16 g) in DMSO (10 g) at 20 °C. Bamboo and wood specimens were respectively placed in conical flasks with 200 mL methanol; then, 4 mL MOF199 precursor solution was added dropwise, and the mixture was stirred for 5 min. The mixture containing bamboo or wood was placed in vacuum for 8 min (−0.08 KPa); then, the vacuum was released and the samples were maintained in air for 8 min. The vacuum/relief cycle was repeated 8 times. After that, portions of the samples were taken out and washed with acetone and ethanol to remove the excess precursor. The above samples were named Bamboo@MOF1 and Wood@MOF1. The remaining samples after treatment with 8 vacuum/relief cycles were immersed in the solution overnight in a vacuum environment and washed with acetone and ethanol; these samples were named Bamboo@MOF2 and Wood@MOF2. Also, the remaining solution was collected and centrifuged to obtain MOF199 crystals. All samples were dried in vacuum at room temperature for 24 h before characterization.

Characterization

Scanning electron microscopy (SEM) images were obtained on a XL30ESEM-FEG (PHILIPS, Netherlands) at 7 kV; the specimens were platinum-coated before imaging. Elemental analysis was performed by energy-dispersive X-ray spectroscopy (EDS, JSM-6480LV, JEOL, Japan). The crystalline structure was analyzed by X-ray diffraction (XRD, X PERTPRO-30X, PHILIPS, Netherlands) at a generator voltage of 40 kV and a generator current of 40 mA with a scanning step size of 0.005° and 0.2 second per step from 5° to 40° under Cu Kα radiation. FT-IR spectra of the MOF199 crystals and MOF199-coated samples were collected with an infrared spectrometer (ANTARIS II, Thermo Fisher, USA) within the range of 4000 to 600 cm^{-1} at a spectral resolution of 4 cm^{-1} and a scanning number of 64. The surface roughnesses of the bamboo and wood samples were measured by an atomic force microscope (AFM, Veeco, USA) in tapping mode with a scan area of 10 μm × 10 μm. The sizes of the crystals on the MOF199-coated samples were statistically calculated using Nano Measurer 1.2 software.

Antibacterial properties

The antibacterial tests were carried out according to the Japan Industry Standard JIS-Z-2801:2000 and Chinese Industry Standard QB/T2591-2003;[22,23] *E. coli* (ATCC 25922) and *S. aureus* (ATCC 6538) were used as test bacteria. The test bacteria were obtained after revitalization of each strain in nutrient broth for 24 hours at 37 ± 1 °C, respectively. After serial dilutions, a final concentration of 5.0 to 10.0 × 10^5 CFU mL^{-1} was obtained. An aliquot of the resulting bacteria suspension (0.2 mL) was then placed onto each sample, where the negative control samples are nutrient broth alone, the blank control samples are the original bamboo and wood, and the antibacterial samples are Bamboo@MOF1, Bamboo@MOF2, Wood@MOF1 and Wood@MOF2, respectively. The samples were respectively covered with polyethylene films (18 × 18 mm^2) and incubated at 37 ± 1 °C for 24 h. After incubation, 20 mL eluent (with 0.5% Tween 80) was used to rinse each sample and polyethylene film. The collected eluent was serially diluted, and aliquots of each dilution were spread on nutrient broth before additional incubation at 37 ± 1 °C for 24 h. The

number of CFUs within the resulting suspensions were calculated according to Chinese Standard GB 4789.2-2016,[24] and three repetitions were tested for each sample. In this work, the actual data are presented as CFU cm^{-2}.

Results and discussion

Crystalline structure

The Bamboo@MOF1 and Wood@MOF1 samples exhibited an aqua blue colour; however, the colours of Bamboo@MOF2 and Wood@MOF2 were much denser (Fig. 1a). The crystalline structures of the deposited crystals on bamboo and wood timber were confirmed by XRD. Fig. 1b presents the XRD pattern of MOF199, which was obtained from the remaining precursor solution. Most of the diffraction peaks (marked with asterisks and stars in Fig. 1b) matched with the MOF199 prepared in other reports;[25] some minor deviations were observed in the relative intensities at certain angles of $2\theta = 8.5°$ and 10.5°, which can be attributed to various degrees of hydration.[26,27] As shown in Fig. 1c and d, there were 3 diffraction peaks at 2θ angles of 16°, 22.5° and 35°, attributed to bamboo and wood. For both the Bamboo@MOF2 and Wood@MOF2 samples (Fig. 1c), the new peaks of 6.6°, 9.5° and 11.5° do not overlap with the diffraction pattern of the original bamboo and are in good agreement with the characteristic peak of MOF199 (marked with asterisks; the enlarged XRD spectra from 6 to 13° are listed in Fig. S1†). The XRD analysis indicated that MOF199 was successfully deposited onto the surfaces of bamboo and wood.

Elemental composition analysis

The surface chemical elemental compositions of Bamboo@MOF2, Wood@MOF2, and the original bamboo and wood were analyzed by EDS. The EDS spectrum of the Bamboo@MOF2 sample is presented in Fig. 2a; C, O, Cu, Pt and Au elements were detected. Meanwhile, Pt and Au elements were ascribed to the coating layer on the samples for SEM analysis. The Cu element originated from the deposited MOF199. The elemental contents of all the coatings can be seen in Fig. 2a (inset); the contents of C, O, Cu and Pt were 34.14%, 47.57%, 10.37% and 7.92% mass, respectively. Four signals from C, O, Cu and Pt were observed in the corresponding EDS spectrum of Wood@MOF2, as shown in the inset in Fig. 2b, which is very similar to Fig. 2a. The contents of C, O, Cu and Pt in Wood@MOF2 were 31.00%, 44.22%, 12.67% and 12.11% mass, respectively. No Cu element was detected in the original bamboo and wood (Fig. S2†), which proves that Cu-MOF is deposited onto the surface of bamboo and wood.

FT-IR analysis

FT-IR measurements were used for further exploring the surface chemical composition changes after MOF deposition. The FT-IR spectrum of MOF199 is shown in Fig. 3a, and the peaks at 730, 761, 1375, 1447, and 1648 cm^{-1} were consistent with the reported chemical structure of MOF199.[28,29] In MOF199, most of the FT-IR characteristic peaks correspond with the organic ligand, benzenetricarboxylic acid. The peak around 3430 cm^{-1} is attributed to the characteristic O–H

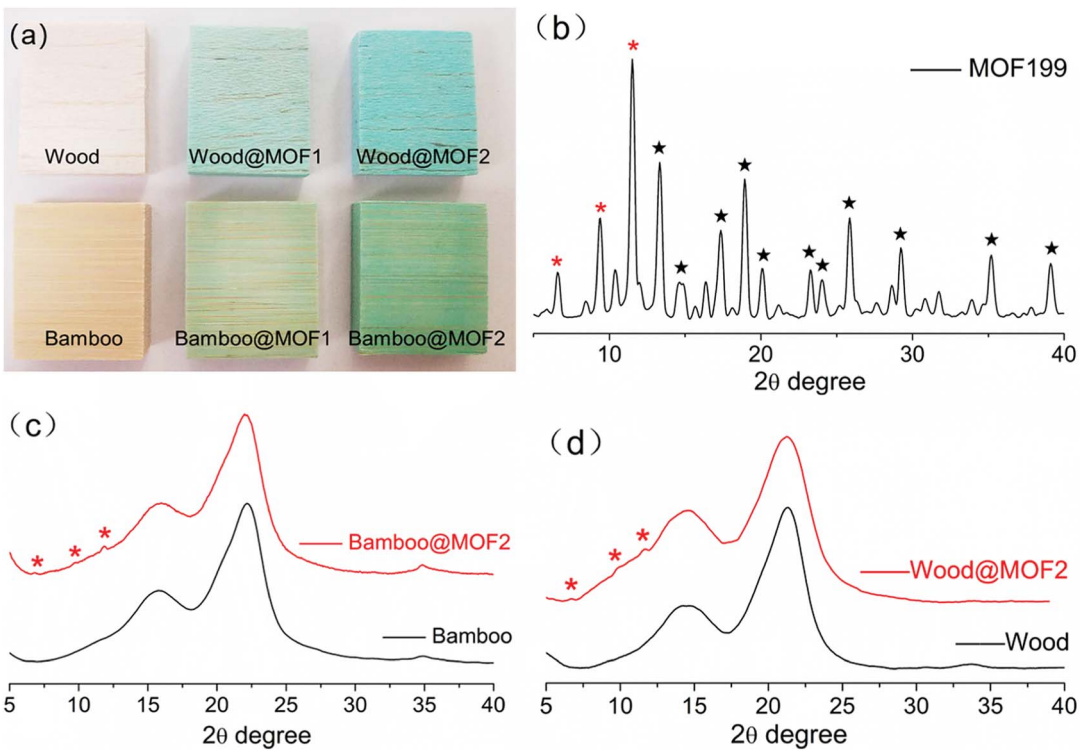

Fig. 1 (a) Optical image of the specimens, (b) XRD spectrum of the synthesized MOF199, (c) XRD spectra of bamboo and Bamboo@MOF2 and (d) XRD spectra of wood and Wood@MOF2.

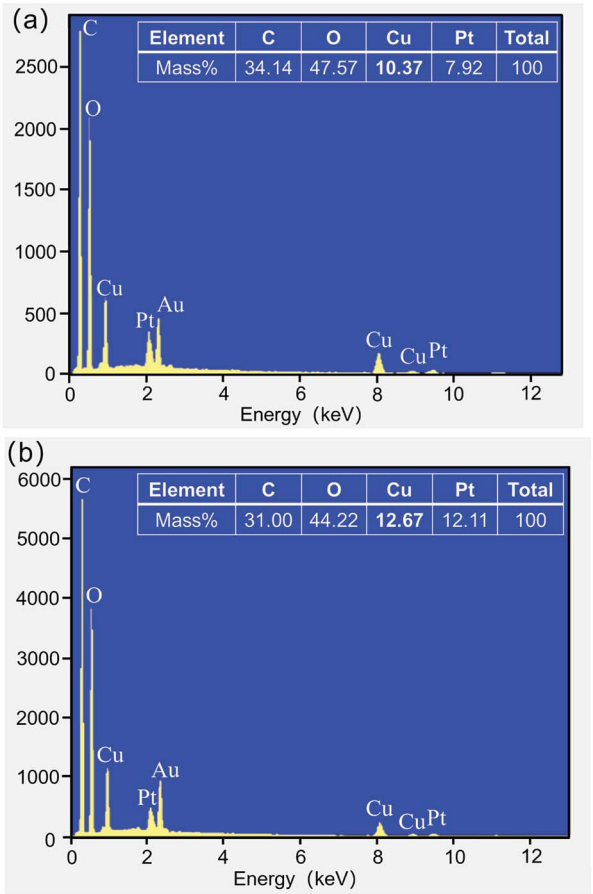

Fig. 2 EDS spectra of (a) Bamboo@MOF2 and (b) Wood@MOF2.

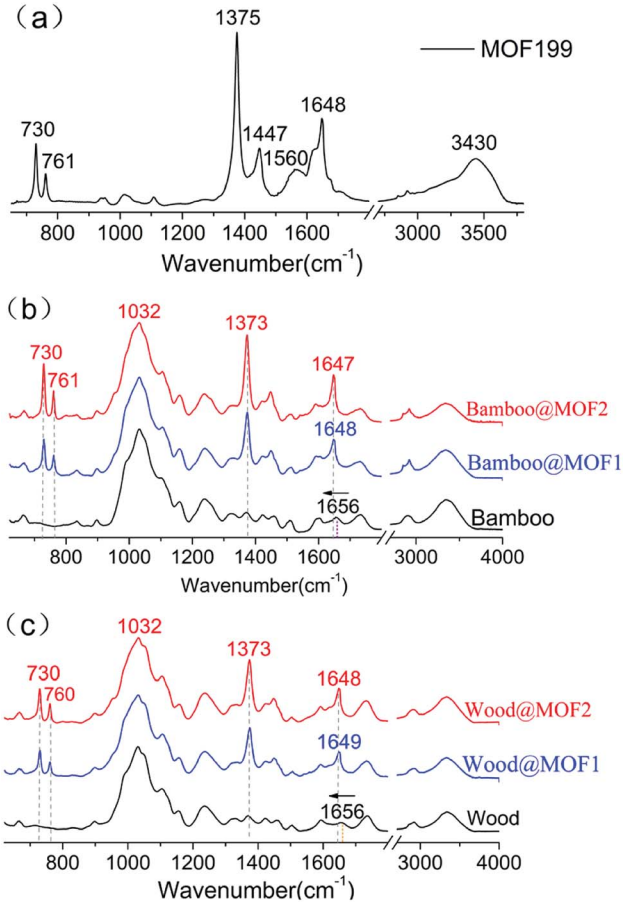

Fig. 3 (a) FTIR spectra of MOF199; (b) ATR-FTIR spectra of bamboo, Bamboo@MOF1 and Bamboo@MOF2; (c) ATR-FTIR spectra of wood, Wood@MOF1, Wood@MOF2.

bonds.[30,31] The peaks at 1648 and 1014 cm^{-1} are due to the C=O and C–O stretching vibrations.[13,32] Absorption bands at 761 and 730 cm^{-1} are attributed to =C–H stretching; the vibration peaks of 1447 and 1375 cm^{-1} are related to the C=C aromatic stretching.[13,33] The FTIR-ATR spectrum of MOF-deposited bamboo and wood are shown in Fig. 3b and c, respectively. After deposition of MOF199 onto bamboo, the original 1656 cm^{-1} peak of the C=O groups disappeared, which is attributed to the lignin structure of bamboo, and a new 1648 cm^{-1} peak appeared with no shoulder side or broadening. However, all the other absorption bands of MOF-deposited bamboo are strongly consistent with those of individual MOF199 and bamboo, as are those of wood. In individual MOF199, the peak of 1648 cm^{-1} is the absorption band of the carboxyl group in benzenetricaboxylic acid, which coordinates with the copper ion; it is reported that metal-carboxylate coordination causes the C=O absorption band to shift to a lower wavelength.[34] Herein, it is speculated that the C=O groups in the lignin structure of bamboo and wood may interact with the copper ion during the deposition, resulting in absorption band shifts and a type of attachment between the MOF199 and the woody substrate. Our absorption band shift results are in agreement with results obtained for similar previously described complexes.[18,32,35]

Morphology

On average, bamboo culm consists of about 52% parenchyma, 40% fiber and 8% conducting tissue (vessels).[7] Bamboo fibers are characterized by thick polylamellate secondary walls, and most of them contain almost no cell lumen.[36] In order to study the *in situ* deposition of the MOF onto the hierarchical surface of the original cell wall in bamboo, the vessels and parenchymal cells of bamboo were chosen for observation because of their larger cell lumen and significant hierarchical structures.

SEM images of the vessels in the original bamboo, Bamboo@MOF1 and Bamboo@MOF2 were obtained. Fig. 4a and d exhibit typical SEM images of the original bamboo vessel surface, which contains numerous pits with the important functions of water and nutrient transportation. For the sample Bamboo@MOF1 (Fig. 4b and e), sparser MOF199 crystals with octahedral crystal structures can be observed on the vessel surface of bamboo. There is also a large number of smaller crystals inside the pits, as shown in the enlargement in Fig. 4f. During the vacuum/relief treatment, the solution of MOF precursor will enter the bamboo through the pits and form crystals inside it; the crystals shown in Fig. 4f retain recognizable octahedral structures. However, the crystal growth is

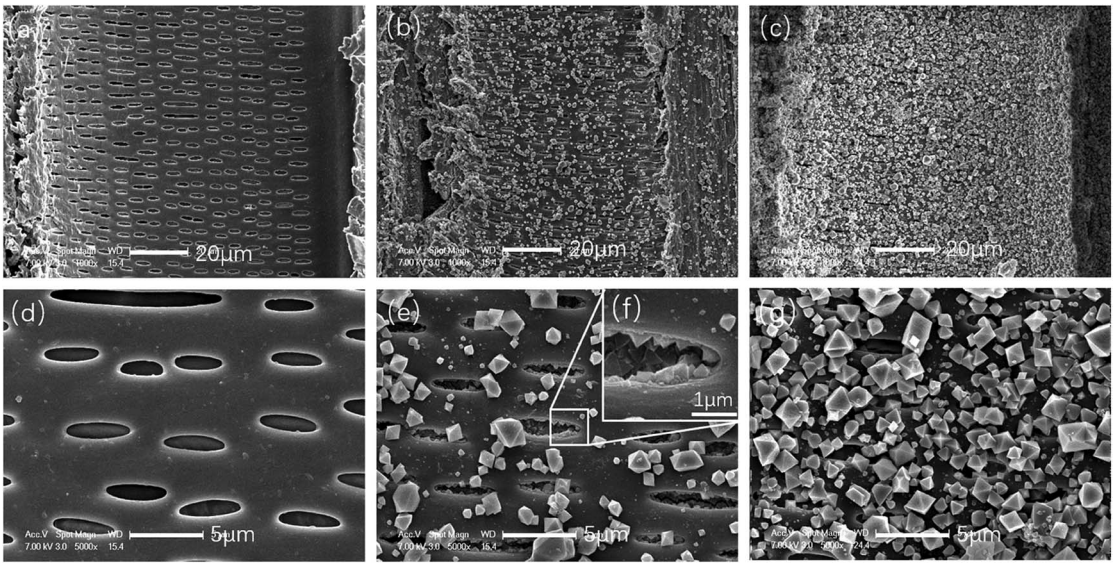

Fig. 4 SEM images of vessels in original bamboo (a and d), Bamboo@MOF1 (b, e and f) and Bamboo@MOF2 (c and g) at different magnifications.

restricted by the limited volume of the pit and results in smaller crystals.[37] For the sample Bamboo@MOF2 (Fig. 4c and g), a large number of MOF199 crystals with uniform sizes are distributed on the vessel surfaces of bamboo, and the pits can barely be distinguished. In Bamboo@MOF2, the overnight immersion prolonged the time of crystal growth and deposition, affording uniform and dense MOF layers. The SEM images show that the vacuum/relief deposition technique is a facile and efficient method for the preparation of MOFs. Also, immersion after vacuum/relief treatment can significantly further improve the deposition.

The deposition of MOF199 on parenchyma cells in the original bamboo was also observed by SEM. As shown in Fig. 5, as with the vessel cells, the vacuum/relief deposition method produced sparser MOF199 crystal layers on the parenchyma cell walls (Fig. 5b and e). The combination of the vacuum/relief deposition method and overnight immersion also led to denser, well-dispersed crystal deposition on the bamboo parenchyma cell surface (Fig. 5c and f).

Unlike bamboo, fiber is the most abundant tissue in balsa wood;[38] therefore, wood fibers were studied by SEM, and images of the original wood, Wood@MOF1, and Wood@MOF2 are shown in Fig. 6. The SEM images in Fig. 6a and d of the original wood fibers show a smooth and uniform surface. In Fig. 6b, the wood surface is coated with a crystal layer, and the magnified image (Fig. 6e) obviously shows MOF199 crystals with uneven

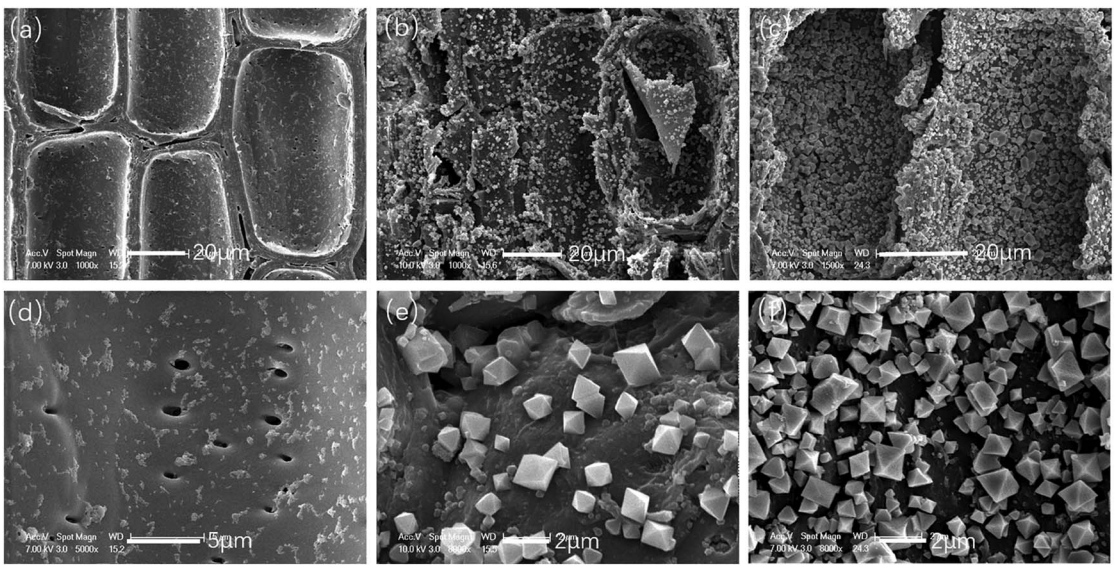

Fig. 5 SEM images of parenchyma cells in original bamboo (a and d), Bamboo@MOF1 (b and e) and Bamboo@MOF2 (c and f) at different magnifications.

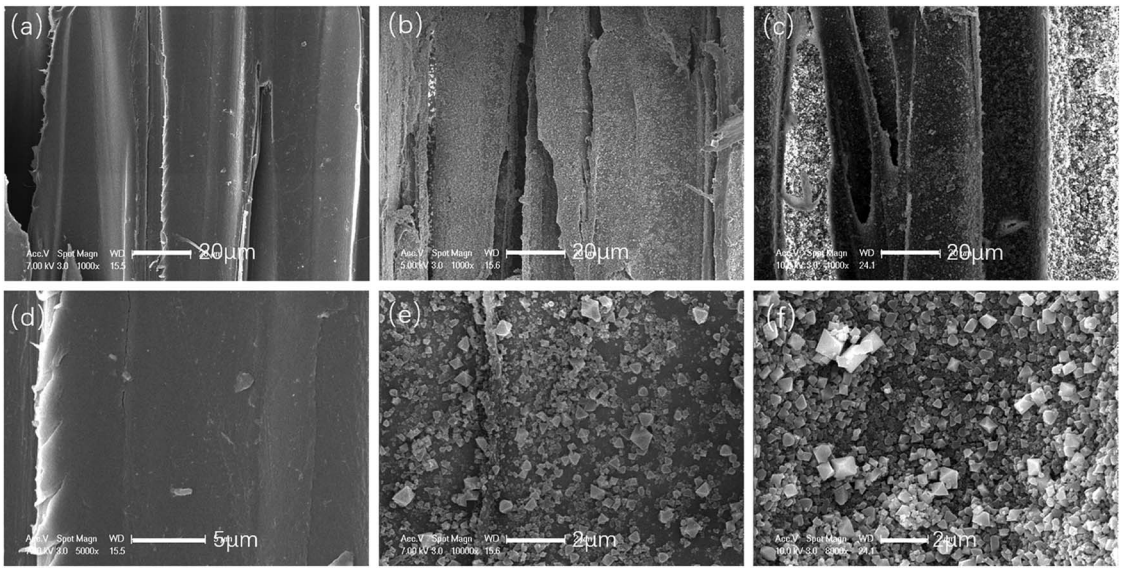

Fig. 6 SEM images of fiber cells in original wood (a and d), Wood@MOF1 (b and e) and Wood@MOF2 (c and f) at different magnifications.

crystal distribution; also, the crystals are smaller than those on the bamboo surface. After overnight immersion, as shown in Fig. 6c and f, the Wood@MOF2 surface is deposited with a much thicker crystal layer, and the magnified SEM image shows a much denser MOF199 crystal layer than that of Wood@MOF1.

From the SEM images, the crystal sizes on bamboo and wood appear to be different. Next, the size distributions of the MOF199 crystals were measured and statistically analyzed by Nano-measurer software according to the enlarged SEM images of Bamboo@MOF2 and Wood@MOF2 in Fig. 4g and 6f. The crystal diameter of bamboo varies from 0.3 μm to 1.8 μm, and the majority vary in size from 0.6 to 0.9 μm, as shown in Fig. 7a. However, the crystal size of Wood@MOF2 was much smaller, and most of the crystal sizes vary in the range from 0.1 to 0.4 μm (Fig. 7b). For both materials, the crystal sizes were smaller than those reported for materials obtained from typical solvothermal synthesis;[28,39] this is attributed to our mild reaction conditions of room temperature and atmospheric pressure. The above crystal size statistics and SEM images suggest that the different surface performance between wood and bamboo may affect the crystal deposition of MOF199.

Surface roughness analysis

A detailed investigation of the surface roughnesses of the original bamboo and wood was performed using AFM to study their effects on the formation of MOF crystals. The 2D and 3D AFM images and cross-sectional height profiles of the bamboo vessels are shown in Fig. 8a, b and c. Several irregular bumps can be found on the surface of the vessel walls. During the growth of bamboo, nutrients and metabolites enter and exit the vessel through the pit, and these substances deposit gradually on the vessel walls; this forms bumps and increases the surface roughness of the vessel (average $R_q = 58.7$ nm).[40] It is difficult for an over-rough surface to trap MOF precursors for nucleation because the surface contains large cavities which are similar to smooth surfaces for the molecules.[37] Therefore, fewer nucleation sites and sufficient space are conducive to the deposition of large MOF crystals.

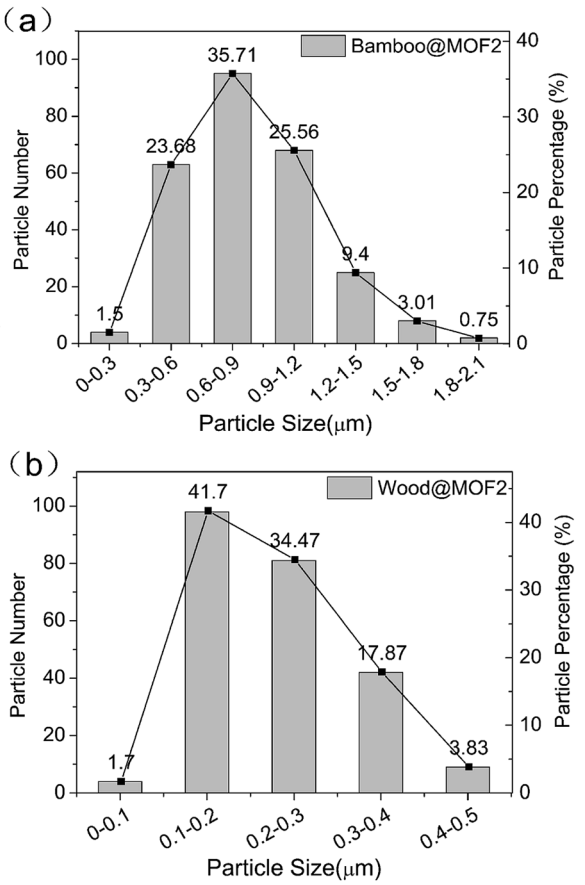

Fig. 7 The sizes of MOF199 crystals on the (a) Bamboo@MOF2 and (b) Wood@MOF2 surfaces.

Fig. 8d, e and f depicts 2D and 3D AFM images and the roughness profile of a parenchyma cell in the original bamboo, obtained from an area of 8.3 μm × 8.3 μm. The AFM images and cross-sectional profiles both reveal a relatively smooth surface, which is consistent with other literature reports;[41] however, the sloping surface and the presence of starch particulate increase the surface roughness (average $R_q = 32.1$ nm). A smooth surface is unfavorable to the nucleation of MOF crystals, leading to larger MOF crystal sizes.

2D, 3D and cross-sectional profiles of a wood fiber are shown in Fig. 8h, i and g, respectively. The 3D images show that the wood fiber has an uneven surface, and the cross-sectional profiles show large numbers of peaks and troughs. However, the value of the surface roughness of the wood fiber (R_q) was 15.6 nm, which is lower than that of the parenchyma cells in bamboo (32.1 nm); this suggests that numerous nano-sized cavities are present on the surface of the wood fiber. The small cavities on the wood surface have appropriate sizes to trap the seed crystals of MOF; this results in rapid nucleation, with high dispersity of the nuclei.[42] However, the limited number of small cavities and the consumption of the precursor by rapid nucleation leads to relatively small MOF crystals on the wood surface.

Antibacterial properties

The antibacterial activities of Bamboo@MOF and Wood@MOF against *E. coli* and *S. aureus* were tested using the antimicrobial plastics method. The growth of *E. coli* and *S. aureus* colonies of the negative control sample (nutrient broth alone), blank control samples (original bamboo and wood), low MOF deposition samples (Bamboo@MOF1 and Wood@MOF1), and high MOF deposition samples (Bamboo@MOF2 and Wood@MOF2) are shown in Fig. 9. The original bamboo and wood showed very low antibacterial activities; bamboo showed slightly better activity than wood because bamboo contains natural antibacterial substances.[43] Bamboo@MOF1 shows improved antibacterial activity compared with the original bamboo; *E. coli* growth decreased from 7.18 to 4.07 CFU cm^{-2}, and *S. aureus* growth decreased further, from 7.1 to 3.41 CFU cm^{-2}. Wood@MOF1 showed similar results; the number of *E. coli* colonies decreased to 5.00 from 7.87 CFU cm^{-2}, and the amount of *S. aureus* decreased to 3.41 from 7.1 CFU cm^{-2}. With a higher content of MOF, the MOF2 samples could minimize the *E. coli* and *S. aureus* colony levels to 2.92 and 2.08 CFU cm^{-2} for bamboo. For balsa wood, the numbers of *E. coli* and *S. aureus* colonies decreased to 3.65 and 2.14 CFU cm^{-2}, respectively. These results indicate that the antibacterial performance increases with the amount of MOF deposition, which is consistent with

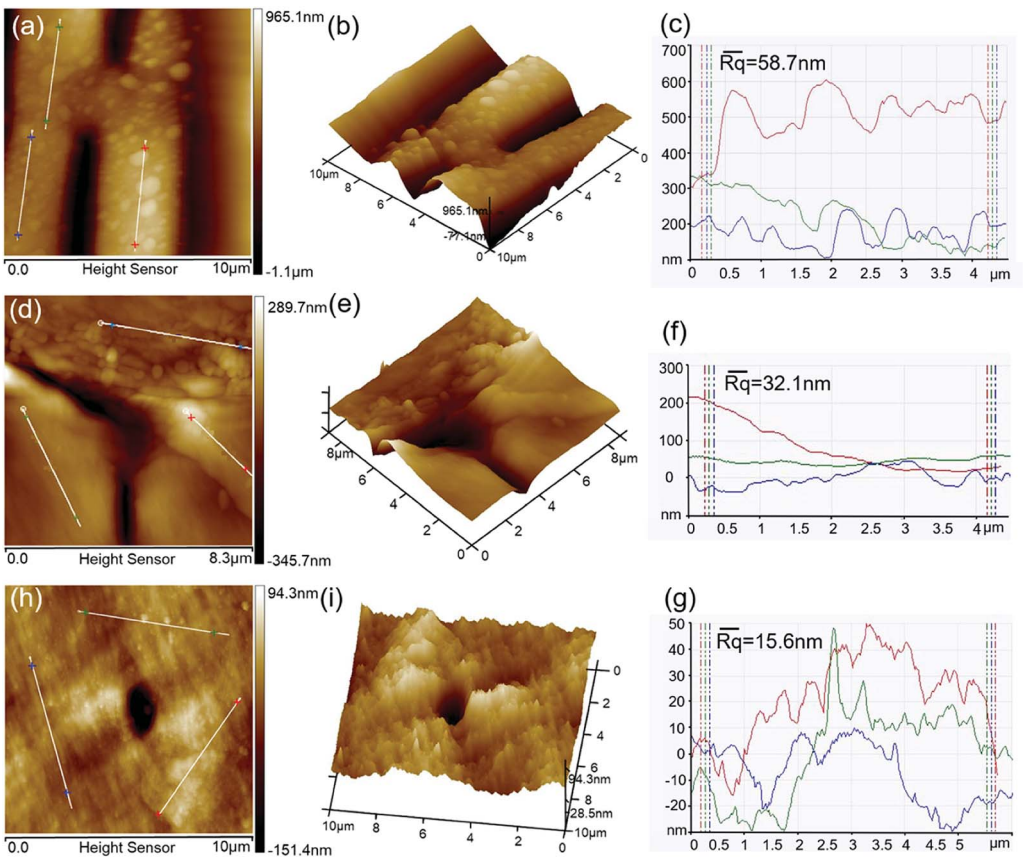

Fig. 8 AFM images of original bamboo and wood timber. 2D, 3D AFM images and cross-sectional height profiles of a vessel cell (a, b and c) and parenchyma cell (d, e and f) in the original bamboo timber, as well as a fiber cell (h, i and g) in the original wood timber. The images are taken from areas of 10 μm × 10 μm (a, b, h and i) and 8.3 μm × 8.3 μm (d and e).

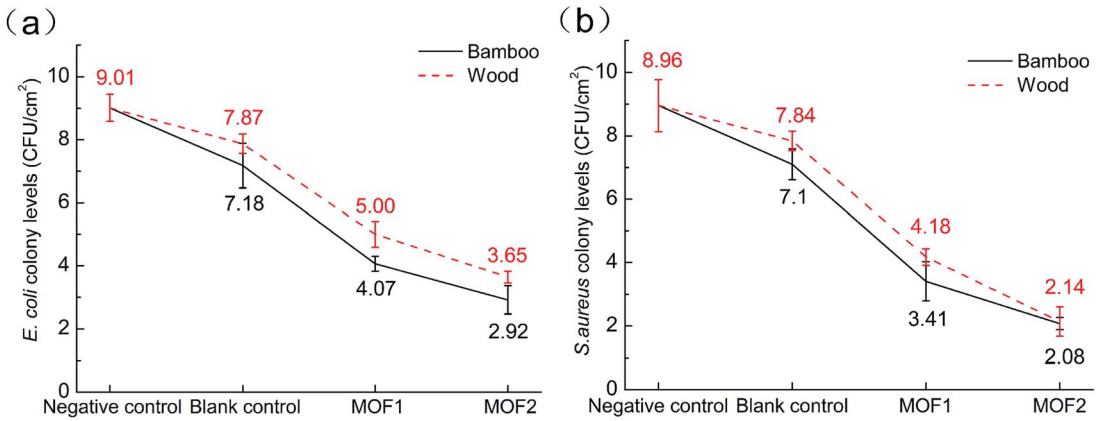

Fig. 9 The bacterial colony levels of (a) *E. coli* and (b) *S. aureus* for the negative control group (nutrient broth alone), blank control samples (original bamboo and wood), MOF1 (Bamboo@MOF1 and Wood@MOF1) samples, and MOF2 (Bamboo@MOF2 and Wood@MOF2) samples after 24 hours of incubation.

the results of MOF199 coated on silk fibers.[18] The result is also consistent with previous studies, in which MOF199-coated materials showed better antibacterial performance against *S. aureus* than *E. coli*; this is due to the more negatively charged surfaces of *S. aureus* cells, which contribute to direct contact interaction with the MOF199-coated samples,[12] and the thicker cell membrane of *E. coli*.[13]

A proposed antibacterial mechanism of the MOF-deposited woody materials is shown in Fig. 10. The deposition of MOF199 endows woody materials with antibacterial activity against both *E. coli* and *S. aureus*. The antimicrobial mechanisms of copper are complex and diverse. Reports have shown that cupric salt-loaded cellulose fibers have no antibacterial activity against either *E. coli* or *S. aureus*,[12] while MOF199 showed significantly improved antimicrobial properties on several different substrates.[12,13,19,20] According to the literature, after being subjected to a microbiological assay for 24 h, the surface of MOF199 was found to be eroded, and copper element appeared in the bacterial cells.[44] The antibacterial behaviour of MOF199 may be caused by the interaction of copper(II) with the cell membrane *via* oxidation of membrane proteins and fatty acids or transmembrane potential alteration, leading to cell lysis.[19] Therefore, we speculate that the MOF on wood/bamboo does not release its metal cations; instead, the bacteria interact with the copper cations on the surface of the MOF, which has adverse impacts on the growth and reproduction of bacteria.[12,45]

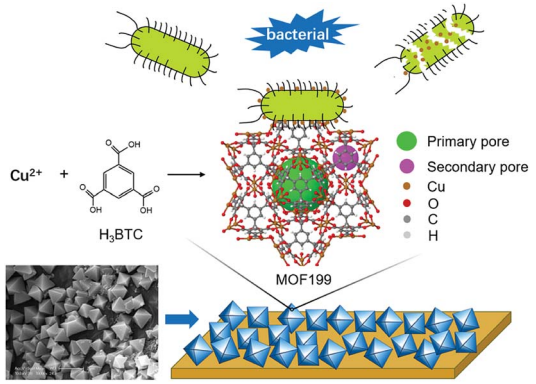

Fig. 10 Schematics of the fabrication of MOF-deposited woody materials and their antibacterial mechanism.

Conclusions

In this study, MOF199 was successfully synthesized on bamboo and wood surfaces by deposition at room temperature. Vacuum/relief cycles combined with overnight immersion treatment were effective to obtain uniform and dense MOF layers. The MOF199 crystals showed relatively large sizes (0.3 to 1.8 μm) on the bamboo surface compared with those on wood surfaces (0.1 to 0.4 μm). The AFM results show that surface roughness is an important factor affecting the crystallization process of MOF199. The low roughness and numerous peaks and troughs of the wood surface results in rapid nucleation with high dispersity of nuclei. Bamboo@MOF and Wood@MOF were both demonstrated to have good antibacterial properties, especially for *S. aureus*. This study provides a new pathway for preparing MOF-coated woody materials with various functions.

Conflicts of interest

There are no conflicts to declare.

Acknowledgements

The work was financially supported by the National Natural Science Foundation of China (Grant No. 31901377) and the Fundamental Research Funds for International Centre for Bamboo and Rattan (No. 1632019016).

Notes and references

1 Y. Liu and G. J. Zhao, *Wooden Resource Materials*, China Forestry Publishers, 2007.

2 J. Li, J. Qiu, Y. X. Liu and H. P. Yu, *Adv. Mater. Res.*, 2010, **113–114**, 1665–1671.
3 T. Li, S. He, W. Gan, Z. Wei, M. Heidarinejad, D. Dalgo, R. Mi, X. Zhao, J. Song, J. Dai, C. Chen, A. Aili, A. Vellore, A. Martini, R. Yang, J. Srebric, X. Yin and L. Hu, *Science*, 2019, **364**, 760–763.
4 Q. Tang, L. Fang, Y. Wang, M. Zou and W. Guo, *Nanoscale*, 2018, **10**, 4344–4352.
5 H. Guan, Z. Cheng and X. Wang, *ACS Nano*, 2018, **12**, 10365–10373.
6 M. Zhu, Y. Li, F. Chen, X. Zhu, J. Dai, Y. Li, Z. Yang, X. Yan, J. Song, Y. Wang, E. Hitz, W. Luo, M. Lu, B. Yang and L. Hu, *Adv. Energy Mater.*, 2017, **8**, 1701028.
7 Z. H. Jiang, *Bamboo and Rattan in the world*, China Forestry Publishers, 2007.
8 J. Li, H. Yu, Z. Wu, J. Wang, S. He, J. Ji, N. Li, Y. Bao, C. Huang, Z. Chen, Y. Chen and C. Jin, *Colloids Surf., A*, 2016, **508**, 117–123.
9 D. Ren, J. Li, J. Xu, Z. Wu, Y. Bao, N. Li and Y. Chen, *Coatings*, 2018, **8**, 341.
10 H. D. Coleman, J.-Y. Park, R. Nair, C. Chapple and S. D. Mansfield, *Proc. Natl. Acad. Sci. U. S. A.*, 2008, **105**, 4501–4506.
11 H. S. Yaddanapudi, N. Hickerson, S. Saini and A. Tiwari, *Vacuum*, 2017, **146**, 649–654.
12 C. Wang, X. Qian and X. An, *Cellulose*, 2015, **22**, 3789–3797.
13 K. Singbumrung, K. Motina, P. Pisitsak, P. Chitichotpanya, S. Wongkasemjit and T. Inprasit, *Fibers Polym.*, 2018, **19**, 1373–1378.
14 I. Perelshtein, G. Applerot, N. Perkas, E. Wehrschuetz-Sigl, A. Hasmann, G. Guebitz and A. Gedanken, *Surf. Coat. Technol.*, 2009, **204**, 54–57.
15 S. Bouson, A. Krittayavathananon, N. Phattharasupakun, P. Siwayaprahm and M. Sawangphruk, *R. Soc. Open Sci.*, 2017, **4**, 170654.
16 H. Guo, E. V. Bachtiar, J. Ribera, M. Heeb, F. W. M. R. Schwarze and I. Burgert, *Green Chem.*, 2018, **20**, 1375–1382.
17 G. Wyszogrodzka, B. Marszalek, B. Gil and P. Dorozynski, *Drug Discovery Today*, 2016, **21**, 1009–1018.
18 A. R. Abbasi, K. Akhbari and A. Morsali, *Ultrason. Sonochem.*, 2012, **19**, 846–852.
19 H. S. Rodríguez, J. P. Hinestroza, C. Ochoa-Puentes, C. A. Sierra and C. Y. Soto, *J. Appl. Polym. Sci.*, 2014, **131**, 40815.
20 M. J. Lis, B. B. Caruzi, G. A. Gil, R. B. Samulewski, A. Bail, F. A. P. Scacchetti, M. P. Moises and F. Maesta Bezerra, *Poly*, 2019, **11**, 713.
21 R. Ameloot, E. Gobechiya, H. Uji-i, J. A. Martens, J. Hofkens, L. Alaerts, B. F. Sels and D. E. De Vos, *Adv. Mater.*, 2010, **22**, 2685–2688.
22 JIS Z2801, Antimicrobial products, Test for antimicrobial activity and efficacy, Japanese industrial standards, 2010.
23 QB/T 2591, Antimicrobial plastics, Test for antimicrobial activity and efficacy, China Light Industry standards, 2003.
24 GB 4789.2, Food Microbiology Testing-Aerobic plate count Determination, China Food Safety Standards, 2016.
25 E. Laurila, J. Thunberg, S. P. Argent, N. R. Champness, S. Zacharias, G. Westman and L. Öhrström, *Adv. Eng. Mater.*, 2015, **17**, 1282–1286.
26 K. Schlichte, T. Kratzke and S. Kaskel, *Microporous Mesoporous Mater.*, 2004, **73**, 81–88.
27 V. K. Saini and J. Pires, *J. Environ. Sci.*, 2017, **55**, 321–330.
28 L. E. Lange and S. K. Obendorf, *ACS Appl. Mater. Interfaces*, 2015, **7**, 3974–3980.
29 J. Song, Z. Luo, D. K. Britt, H. Furukawa, O. M. Yaghi, K. I. Hardcastle and C. L. Hill, *J. Am. Chem. Soc.*, 2011, **133**, 16839–16846.
30 D. Ren, J. Li, Y. Bao, Z. Wu, S. He, A. Wang, F. Guo and Y. Chen, *Colloids Surf., A*, 2018, **555**, 381–388.
31 S. Loera-Serna, M. A. Oliver-Tolentino, M. de Lourdes López-Núñez, A. Santana-Cruz, A. Guzmán-Vargas, R. Cabrera-Sierra, H. I. Beltrán and J. Flores, *J. Alloys Compd.*, 2012, **540**, 113–120.
32 R. M. Abdelhameed, H. Abdel-Gawad, M. Elshahat and H. E. Emam, *RSC Adv.*, 2016, **6**, 42324–42333.
33 P. C. Lemaire, J. Zhao, P. S. Williams, H. J. Walls, S. D. Shepherd, M. D. Losego, G. W. Peterson and G. N. Parsons, *ACS Appl. Mater. Interfaces*, 2016, **8**, 9514–9522.
34 S. K. Papageorgiou, E. P. Kouvelos, E. P. Favvas, A. A. Sapalidis, G. E. Romanos and F. K. Katsaros, *Carbohydr. Res.*, 2010, **345**, 469–473.
35 H. E. Emam, N. H. Saleh, K. S. Nagy and M. K. Zahran, *Int. J. Biol. Macromol.*, 2016, **84**, 308–318.
36 C. H. Cho, K. H. Lee, J. S. Kim and Y. S. Kim, *J. Wood Sci.*, 2008, **54**, 261–265.
37 H. Hou, B. Wang, S.-Y. Hu, M.-Y. Wang, J. Feng, P.-P. Xie and D.-C. Yin, *J. Cryst. Growth*, 2017, **468**, 290–294.
38 R. Ameloot, E. Gobechiya, H. Uji-i, J. A. Martens, J. Hofkens, L. Alaerts, B. F. Sels and D. E. De Vos, *Adv. Mater.*, 2010, **22**, 2685–2688.
39 M. Schlesinger, S. Schulze, M. Hietschold and M. Mehring, *Microporous Mesoporous Mater.*, 2010, **132**, 121–127.
40 R. Liu, S. Yang, H. Li, Z. Zhai and B. Fei, *J. Nanjing For. Univ.*, 2017, **41**, 163–168.
41 J. Li, Z. Wu, Y. Bao, Y. Chen, C. Huang, N. Li, S. He and Z. Chen, *J. Saudi Chem. Soc.*, 2017, **21**, 920–928.
42 S. Ramachandran and A. Sivasamy, *Int. J. Nanosci.*, 2017, **17**, 1760008.
43 T. Afrin, T. Tsuzuki, R. K. Kanwar and X. Wang, *J. Text. Inst.*, 2012, **103**, 844–849.
44 C. Chiericatti, J. C. Basilico, M. L. Zapata Basilico and J. M. Zamaro, *Microporous Mesoporous Mater.*, 2012, **162**, 60–63.
45 S. Ma, M. Zhang, J. Nie, B. Yang, S. Song and P. Lu, *Cellulose*, 2018, **25**, 5999–6010.